Published in final edited form as:
Mol Pharm. 2013 July 1; 10(7): 2730–2738. doi:10.1021/mp4001662.

Synergistic Combination of Small Molecule Inhibitor and RNA interference Against Anti-apoptotic Bcl-2 Protein in Head and Neck Cancer Cells

Yen-Ling Lin[a], **Yasemin Yuksel Durmaz**[a], **Jacques E. Nör**[b], and **Mohamed E. H. ElSayed**[a,c,*]

[a]University of Michigan, College of Engineering, Department of Biomedical Engineering, Cellular Engineering & Nano-Therapeutics Laboratory, Ann Arbor, MI, 48109, USA

[b]University of Michigan, School of Dentistry, Department of Cariology, Restorative Sciences, and Endodontics, Ann Arbor, MI, 48109, USA

[c]University of Michigan, Macromolecular Science and Engineering Program, Ann Arbor, MI, 48109, USA

Abstract

B-cell lymphoma 2 (Bcl-2) is an anti-apoptotic protein that is over-expressed in head and neck squamous cell carcinomas, which has been implicated in development of radio- and chemo-resistance. Small molecule inhibitors such as AT-101 (a BH3-mimetic drug) have been developed to inhibit the anti-apoptotic activity of Bcl-2 proteins, which proved effective in restoring radio- and chemo-sensitivity in head and neck cancer cells. However, high doses of AT-101 are associated with gastrointestinal, hepatic, and fertility side effects, which prompted the search for other Bcl-2 inhibitors. Short interfering RNA (siRNA) proved to inhibit anti-apoptotic Bcl-2 protein expression and trigger cancer cell death. However, transforming siRNA molecules into a viable therapy remains a challenge due to the lack of efficient and biocompatible carriers. We report the development of degradable star-shaped polymers that proved to condense anti-Bcl-2 siRNA into “smart” pH-sensitive and membrane-destabilizing particles that shuttle their cargo past the endosomal membrane and into the cytoplasm of head and neck cancer cells. Results show that “smart” anti-Bcl-2 particles reduced the mRNA and protein levels of anti-apoptotic Bcl-2 protein in UM-SCC-17B cancer cells by 50-60% and 65-75%, respectively. Results also show that combining “smart” anti-Bcl-2 particles with the IC_{25} of AT-101 (inhibitory concentration responsible for killing 25% of the cells) synergistically inhibit cancer cell proliferation and increase cell apoptosis, which reduced the survival of UM-SCC-17B cancer cells compared to treatment with AT-101 alone. Results indicate the therapeutic benefit of combining siRNA-mediated knockdown of anti-apoptotic Bcl-2 protein expression with low doses of AT-101 for inhibiting the growth of head and neck cancer cells.

[*]Corresponding Author: Mohamed E.H. ElSayed, Ph.D., University of Michigan, Department of Biomedical Engineering, 1101 Beal Avenue, Lurie Biomedical Engineering Building, Room 2150, Ann Arbor, MI 48109, USA, Phone: + 1 (734) 615-9404, Fax: + 1 (734) 647-4834, melsayed@umich.edu, Web: www.bme.umich.edu/centlab.php.

Keywords

"Smart" particles; Bcl-2 knockdown; AT-101 inhibitor; Drug delivery

Introduction

Head and neck cancer is a commonly diagnosed cancer that accounts for approximately 650,000 new cases and 350,000 cancer-related deaths worldwide every year.[1] The five-year survival of head and neck cancer at all stages is 50-60%, which is one of the lowest survival rates among all cancers.[2] Treatment of head and neck cancer with a combination of radio- and chemotherapy has improved patient's outcome compared to radiotherapy alone.[3, 4] However, the efficacy of both radio- and chemotherapy is highly limited by the emergence of resistant cancer cells.[5-8] Therefore, it is important to develop an effective strategy to restore the sensitivity of head and neck cancer cells to radio- and chemotherapy.

B-cell lymphoma 2 (Bcl-2) is a family of proteins that includes more than 20 apoptotic regulators with opposing functions but share at least one conserved Bcl-2 homology (BH) domain.[9-11] Anti-apoptotic proteins such as Bcl-2, Bcl-X_L, and Bcl-w appear to inhibit apoptotic cell death through their binding to the pro-apoptotic proteins.[9-11] Pro-apoptotic proteins are sub-grouped into the "Bax" family proteins, which have several domains that are homologous to the domains of anti-apoptotic proteins.[9-11] The "BH3-only" family proteins have the BH3 domain that is conserved in anti-apoptotic proteins.[9-11] In response to the death signal, "Bax" family proteins such as Bax and Bak form homo-oligomers on the mitochondrial membrane, which result in the cytoplasmic release of cytochrome c and initiating the caspase cascade that eventually leads to apoptotic cell death.[9-11] In comparison, Bcl-2 is a pro-survival protein that is over-expressed in multiple human cancer cells including head and neck cancer, which prevents cancer cell death.[12, 13] The anti-apoptotic activity of Bcl-2 protein is attributed to its ability to stabilize the mitochondrial membrane and inhibit the cytoplasmic release of cytochrome c, which prevents the activation of caspases and initiation of cell apoptosis.[13, 14] Overexpression of anti-apoptotic Bcl-2 protein in head and neck cancer cells has been linked to increased resistance to radio- and chemotherapy and is considered a viable therapeutic target.[15, 16]

Several small molecule inhibitors have been developed to inhibit the anti-apoptotic activity of Bcl-2 proteins as a strategy to restore radio- and chemo-sensitivity in head and neck cancer cells.[17] For example, AT-101 is a BH3-mimetic drug extracted from cotton seed oil that proved to induce apoptosis in head and neck cancer cells by binding to the BH3 domain of anti-apoptotic Bcl-2 protein, which restored cancer cell sensitivity to anticancer drugs.[18] However, clinical use of AT-101 was associated with gastrointestinal side effects including intestinal obstruction, which increased with the increase in AT-101 dose.[19] Furthermore, the use of AT-101 in preclinical cancer models was associated with inhibition of spermatogenesis and significant hepatic toxicity at high doses, which motivated the search for other Bcl-2 inhibitors.[20-23] Another strategy relies on antisense oligodeoxynucleotides (ASODN) and short hairpin RNA (shRNA) molecules to silence the expression of anti-apoptotic Bcl-2 protein in head and neck cancer cells, which proved to successfully induce

cancer cell death in response to chemotherapy both *in vitro* and *in vivo*.[24, 25] These studies clearly show that blocking the activity of anti-apoptotic Bcl-2 protein inhibits tumor growth and restores cancer cell sensitivity to anticancer drugs.

In this paper, we report the development of "smart" particles that successfully shuttle silencing RNA (siRNA) molecules past the endosomal membrane and into the cytoplasm of UM-SCC-17B head and neck cancer cells to knockdown the expression of anti-apoptotic Bcl-2 protein. Specifically, we have designed and synthesized a new degradable, star-shaped, pH-sensitive, and membrane-destabilizing polymer[26] that condense anti-Bcl-2 siRNA molecules into "smart" pH-sensitive nanoparticles. This star-shaped polymer is composed of a random copolymer of hydrophobic hexyl methacrylate (HMA) and pH-sensitive 2-(dimethylamino)ethyl methacrylate (DMAEMA) monomers (50/50 molar feed ratio) grafted to the secondary face of the β-cyclodextrin (β-CD) core via acid-labile hydrazone linkages. We quaternized 50% of DMAEMA monomers into cationic N,N,N-trimethylaminoethyl methacrylate iodide (TMAEMA) to allow efficient complexation of anti-Bcl-2 siRNA molecules via electrostatic interaction between cationic nitrogen (N) groups of the polymer and anionic phosphate (P) groups of the siRNA molecules forming "smart" pH-sensitive and membrane-destabilizing particles (Figure 1). "Smart" particles prepared using the β-CD-P(HMA-*co*-DMAEMA-*co*-TMAEMA)$_{4.8}$ polymer are stable at physiologic pH and enter UM-SCC-17B cancer cells via endocytosis.[26] In the endosome, acid-labile hydrazone linkages are hydrolyzed in response to acidic endosomal pH and release the membrane active P(HMA-*co*-DMAEMA-*co*-TMAEMA) grafts, which rupture the endosomal membrane and release the loaded siRNA cargo into the cytoplasm.[26] We report the ability of β-CD-P(HMA-*co*-DMAEMA-*co*-TMAEMA)$_{4.8}$ polymer to condense anti-Bcl-2 siRNA into "smart" particles that deliver their cargo past the endosomal membrane and into the cytoplasm of UM-SCC-17B cancer cells to achieve efficient Bcl-2 knockdown at the mRNA and protein levels. Further, we report the synergistic anticancer activity of siRNA-mediated Bcl-2 knockdown when combined with AT-101 (small molecule inhibitor), which indicate the therapeutic potential of this combination for treatment of head and neck cancer.

Materials and Methods

Materials

β-Cyclodextrin (Aldrich, 98 %) was freeze-dried before use. 2-(dimethylamino)ethyl methacrylate (Aldrich, 98 %) and hexyl methacrylate (Aldrich, 98 %) were passed through basic alumina column to remove the associated inhibitor before use. 1,1,4,7,10,10-Hexamethyltriethylenetetramine (HMTETA) as a ligand (Aldrich, 97 %) was distilled before use. 2-Bromo-2-methyl-propionic acid 4-formyl-phenyl ester (Ald-Br) was synthesized following a published protocol.[27] Copper (I) chloride (CuCl) (Aldrich, 99.9 %), copper (II) chloride ($CuCl_2$) (Aldrich, 99.9%), *tert*-butyldimethylsilyl chloride (TBDMS) (Aldrich, 97%), phenyl bromoacetate (Aldrich, 98%), sodium hydride (NaH) (Aldrich, 60% dispersion in mineral oil), hydrazine anhydrous (Aldrich, 98%), pyridine anhydrous (Aldrich, 98%), 2-bromoisobutyryl bromide (Fluka, > 97%), tetrabutylammonium floride 1.0 M solution in tetrahydrofuran (TBAF) (Aldrich), iodomethane (Aldrich, 99%),

tetrahydrofuran anhydrous (THF) (Aldrich, > 99.9 %) were used as received. Trichloroacetic acid, trizma base, and sulforhodamine B solium salt were purchased from Sigma-Aldrich (St. Louis, MO). Propidium iodide was purchased from MP Biomedicals (Santa Ana, CA). The Bcl-2 siRNA sequence (5′-GCCCUGAUUGUGUAUAUUCA-3′) was synthesized by Integrated DNA Technologies, Inc. (Coralville, Iowa). Scrambled siRNA molecules were purchased from Ambion Inc. (Austin, TX). The RNeasy Mini Kit and Omniscript reverse transcriptase kit were purchased from Qiagen (Valencia, CA). The TaqMan universal PCR master mix and TaqMan gene expression assays for human Bcl-2 and 18S rRNA genes were purchased from Applied Biosystems (Foster, CA). The anti-human β-actin monoclonal antibody and anti-human Bcl-2 monoclonal antibody were purchased from Santa Cruz Biotechnology (Santa Cruz, CA) and BD Biosciences (San Jose, CA), respectively. The AT-101 was purchased from Tocris Bioscience (Minneapolis, MN).

Synthesis of Star-shaped, pH-sensitive, Membrane-destabilizing polymer

The star-shaped β-CD-P(HMA-*co*-DMAEMA-*co*-TMAEMA)$_{4.8}$ polymer was synthesized following our established protocol.[26] Specifically, we utilized the asymmetric distribution of primary hydroxyl groups on the primary face and secondary hydroxyl groups on the secondary face of the β-CD core to graft amphiphilic P(HMA-*co*-DMAEMA) polymer from the secondary face via acid-labile hydrazone linkages using atom transfer radical polymerization (ATRP). Briefly, we used *tert*-butyldimethylsilyl chloride (TBDMSCl) to cap 96% of the primary hydroxyl groups forming (TBDMS)$_7$-β-CD (compound **2**), which allowed us to selectively modify the secondary hydroxyl groups in subsequent reactions (Figure S1, Supplementary Data). The average number of secondary hydroxyl groups that reacted with phenyl acetate was 8.5 yielding (TBDMS)$_7$-β-CD-(phenyl acetate)$_{8.5}$ (compound **3**), which was completely (100%) transformed to the corresponding acyl hydrazide (TBDMS)$_7$-β-CD-(hydrazide)$_{8.5}$ (compound **4**). We utilized the aromatic protons of the phenyl groups to quantitatively confirm the formation of the phenyl acetate ester and subsequent transformation to the acyl hydrazide based on the ^{1}H NMR spectra (Figures S2-S4, Supplementary Data). We reacted (TBDMS)$_7$-β-CD-(hydrazide)$_{8.5}$ (compound **4**) with 2-bromo-2-methyl-propionic acid-4-formyl-phenyl ester (compound **5**) to introduce the initiation sites for ATRP conjugation via acid-labile hydrazone linkages to the β-CD secondary face following published protocols.[28-30] By comparing the ratio between TBDMS and the aromatic protons in the (TBDMS)$_7$-β-CD-(hydrazone-Br)$_{4.8}$ (compound **6**), we confirmed the conjugation of 4.8 ATRP initiation sites (Figure S5, Supplementary Data), which is sufficient for grafting the desired number of cationic groups for condensation of a large dose of siRNA molecules without causing undesirable gelation of the star polymers at higher grafting densities.

We used (TBDMS)$_7$-β-CD-(hydrazone-Br)$_{4.8}$ (Compound **6**) as a macroinitiator for copolymerization of HMA and DMAEMA monomers using the CuCl/CuCl$_2$/HMATETA catalytic system in tetrahydrofuran at 60 °C, which yielded a (TBDMS)$_7$-β-CD-P(HMA-*co*-**D**MAEMA)$_{4.8}$ star polymer with HMA/DMAEMA ratio of 50/50 and graft's average molecular weight of 25 kDa. Graft composition was confirmed based on the corresponding ^{1}H NMR spectrum (Figure S6A, Supplementary Data). The TBDMS protecting groups were removed to yield β-CD-P(HMA-*co*-**D**MAEMA)$_{4.8}$ (compound **7**)

star polymer before quaternization of 50% of the DMAEMA monomers into N,N,N-trimethylaminoethyl methacrylate iodide (TMAEMA) using methylene iodide to obtain β-CD-P(HMA-*co*-**D**MAEMA-*co*-**T**MAEMA)$_{4.8}$ polymer (compound **8**). As shown in Figure S6B (Supplementary Data), we used the ratio between the methyl protons of the DMAEMA monomers at 2.26 ppm and those of the TMAEMA monomers at 3.61 ppm to confirm the % of quaternized DMAEMA monomers.

Cell Culture

UM-SCC-17B cancer cells were cultured following established protocols.[26] Briefly, UM-SCC-17B cells were maintained in DMEM culture medium supplemented with 10% fetal bovine serum, 10,000 units/mL penicillin, and 10,000 μg/mL streptomycin while regularly changing the culture medium every 2 days. Cells were incubated at 37 °C, 5% CO_2, 95% relative humidity, and passaged upon reaching 70-90% confluence using 0.25% trypsin/EDTA mixture.

In vitro Effect of "smart" Anti-Bcl-2 Particles

β-CD-P(HMA-*co*-DMAEMA-*co*-TMAEMA)$_{4.8}$ polymer (1.925 μg) was dissolved in 5.776 μL RNase-free water and mixed with 0.57 μg of anti-Bcl-2 or scrambled siRNA (control) dissolved in 0.8 μL RNase-free water at N/P ratio of 2.5/1 for 20 minutes to prepare anti-Bcl-2 and scrambled "smart" particles, respectively. UM-SCC-17B cells were plated in 24-well plates at a seeding density of 20,000 cells/ well and allowed to adhere for 18 hours before adding anti-Bcl-2 or scrambled "smart" particles at a final siRNA concentration of 100 nM and incubating in serum-free OPTI-MEM medium for 6 hours. Fresh culture medium (500 μL) was added to treated cells followed by incubation for a total of 48 and 72 hours before assaying the change in Bcl-2 expression at the mRNA and protein levels. For quantification of Bcl-2 mRNA level, total RNA was isolated from UM-SCC-17B cells using the RNeasy Mini Kit (Qiagen Inc, Valencia, CA) and 0.25 μg of total RNA was reverse transcribed using Omniscript reverse transcriptase kit (Qiagen Inc, Valencia, CA) following manufacturer's protocols. Real-time PCR was performed in a final volume of 20 μL containing 2 μL of cDNA (corresponding to 10 ng of total RNA for Bcl-2 and 18S rRNA amplification), 1 μL of each primer, and 10 μL of the qPCR MasterMix in the 7500 Fast Real-Time PCR system (Life Technologies, Grand Island, NY). Change in the amount of Bcl-2 protein expressed by treated UM-SCC-17B cells was quantified using western blotting technique following established protocol.[31] Briefly, whole cell lysates were resolved by SDS-PAGE and the membranes were probed overnight at 4°C with anti-human β-actin monoclonal antibody (1:1000000) and anti-human Bcl-2 monoclonal antibody (1:1000) before visualizing both proteins using the SuperSignal West Pico Chemiluminescent Substrate (Pierce, Rockford, IL). Five replicates were used for each condition in each experiment. The knockdown of Bcl-2 protein expression in response to different treatments was quantified using Image J software (NIH, Bethesda, MD) and normalized to that of untreated UM-SCC-17B cells (negative control).

Effect of AT-101 on Cancer Cell Survival

UM-SCC-17B cells were plated in 24-well plates at a seeding density of 10,000 cells/ well and allowed to adhere for 18 hours before incubating with different concentrations (0.1-8 μM) of AT-101 for 48 and 72 hours. Cell survival was examined using the sulforhodamine B (SRB) assay following an established protocol.[18] Briefly, UM-SCC-17B cells were fixed by incubation with 10% trichloroacetic acid (final concentration) for 1 hour at 4°C before staining cellular proteins using 0.4% SRB in 1% acetic acid for 30 minutes at room temperature. Unbound SRB was removed by washing with 1% acetic acid and treated plates were allowed to air dry. Bound SRB was resolubilized in 10 mM Tris base followed by measuring UV absorbance at 565 nm using a Fluoroskan plate reader (Thermo scientific, Asheville, NC). Survival of UM-SCC-17B cells in response to different AT-101 concentrations was normalized to the initial cell plating density and to that observed upon incubation in drug-free culture medium. Using SRB assay, we determined the IC_{25}, IC_{50}, and IC_{75} of AT-101 on UM-SCC-17B cells upon incubation for 48 and 72 hours. Five replicates were used for each condition in each experiment.

Combined Treatment with "Smart" Anti-Bcl-2 Particles and AT-101

We investigated the effect of treating UM-SCC-17B cells with the IC_{25} of AT-101 alone and in combination with "smart" nanoparticles loaded with 0.57 μg of anti-Bcl-2 or scrambled siRNA on cell's viability and apoptotic death using the SRB assay and propidium iodide (PI) staining, respectively. Briefly, UM-SCC-17B cells were plated in 24-well plates at a seeding density of 10,000 cells/ well and allowed to adhere for 18 hours before incubation with different treatments. "Smart" anti-Bcl-2 or scrambled particles were incubated with UM-SCC-17B cells at a final siRNA concentration of 100 nM for 6 hours before adding 500 μL of fresh culture medium containing the AT-101 and incubating for a total of 72 hours. Cell survival was determined by the SRB assay following the protocol described earlier.[18] To measure cell apoptosis in response to different treatments, cells were treated with 0.25% trypsin/EDTA solution, harvested, and centrifuged to remove the supernatant and form a cell pellet before suspending the pellets in PBS and incubating with PI for 20 minutes. The fractions of apoptotic cells and in different phases of the cell cycle were measured using flow cytometry (Biosciences FACSCalibur, Becton Dickinson, Franklin Lakes, NJ). Five replicates were used for each condition in each experiment. We calculated the Combinatorial Index (CI) using CalcuSyn Software (Biosoft, Cambridge, UK) to determine the nature of the combined effect of AT-101 and "smart" particles on UM-SCC-17B survival where $CI < 0.9$ indicates a synergistic effect, $0.9 \leq CI \leq 1.1$ indicates an additive effect, and $CI > 1.1$ indicates the lack of a combinatorial effect.

Results and Discussion

In Vitro Effect of "Smart" Anti-Bcl-2 Particles

Star-shaped β-CD-P(HMA-*co*-DMAEMA-*co*-TMAEMA)$_{4.8}$ polymer was successfully synthesized and proved to complex anti-Bcl-2 siRNA molecules forming "smart" nanoparticles at N/P ratio of 2.5/1.[26] We investigated the ability of "smart" particles to deliver functional anti-Bcl-2 siRNA molecules past the endosomal membrane and into the cytoplasm of UM-SCC-17B head and neck cells based on their ability to selectively

knockdown Bcl-2 gene expression at both the mRNA and protein levels compared to "smart" particles loaded with a scrambled siRNA sequence. Earlier reports showed that antisense oligodeoxynucleotides knockdown Bcl-2 expression within 48-72 hours of the treatment followed by a gradual recovery in Bcl-2 expression after 96 hours.[32] Therefore, we chose to evaluate the effect of "smart" particles loaded with anti-Bcl-2 siRNA after 48 and 72 hours from their incubation with UM-SCC-17B cells compared to "smart" particles loaded with scrambled siRNA. Results show that "smart" particles loaded with anti-Bcl-2 siRNA selectively knocked down the Bcl-2 mRNA level in UM-SCC-17B cells by 60% and 50% after 48 and 72 hours, respectively (Figure 2A). "Smart" anti-Bcl-2 particles similarly reduced Bcl-2 protein level in UM-SCC-17B cells by 66% and 76% after 48 and 72 hours, respectively (Figure 2B). "Smart" particles loaded with scrambled siRNA sequence did not affect Bcl-2 expression, which indicates the selectivity and biocompatibility of anti-Bcl-2 particles.

Effect of AT-101 on Cell Survival

We investigated the viability of UM-SCC-17B cancer cells upon incubation with AT-101 for 48 and 72 hours as a function of AT-101 concentration (0, 0.1, 0.5, 1, 2, 4, and 8 μM) using the SRB assay. Results show a typical sigmoidal relationship between cancer cell survival and the concentration of AT-101 inhibitor where the percentage of viable cells decreased with the increase in AT-101 concentration (Figure 3). Results show that AT-101 concentration required to kill 25% (IC_{25}), 50% (IC_{50}), and 75% (IC_{75}) of UM-SCC-17B cancer cells depends on the incubation time (48 versus 72 hours). Specifically, results show that the IC_{25}, IC_{50}, and IC_{75} of AT-101 are 2.88, 4.87, and 6.63 μM upon incubation with UM-SCC-17B cancer cells for 48 hours (Figure 3A). In comparison, the IC_{25}, IC_{50}, and IC_{75} of AT-101 decrease to 1.69, 2.51, and 3.63 μM upon incubation with UM-SCC-17B cancer cells for 72 hours (Figure 3B). The observed IC_{50} after 48 and 72 hours is similar to the reported values in previous studies.[18] However, western blots show that incubation of UM-SCC-17B cancer cells with the IC_{25} and IC_{50} of AT-101 for 48 and 72 hours did not affect the expression levels of Bcl-2 protein compared to untreated cells (Figure 3C).

Results show that treatment of UM-SCC-17B cancer cells with AT-101 inhibitor triggered apoptosis that was quantified by PI staining (Figure 4). Specifically, incubation of UM-SCC-17B cells with the IC_{25}, IC_{50}, and IC_{75} of AT-101 for 48 hours increased the fraction of apoptotic cancer cells from 1% observed with untreated cells (control) to 4, 8, and 21%, respectively (Figure 4A). Increasing the incubation time to 72 hours increased the fraction of apoptotic cancer cells from 2% for untreated cells (control) to 5, 30, and 47%, respectively (Figure 4A). The ability of AT-101 to trigger apoptosis of UM-SCC-17B cancer cells is a result of its ability to compete with the BH3 protein for the binding groove of anti-apoptotic Bcl-2 proteins, which blocks the dimerization of Bcl-2 proteins with pro-apoptotic ones such as Bak and Bax thus allowing the cells to undergo apoptosis.[33, 34] Careful analysis of the cell cycle of treated cells shows that treatment with AT-101 arrested cell cycle in the G_1 phase (Figures 4B & 4C) and inhibited cell mitosis indicated by the decrease in the mitotic index (fraction of cells in S and G2 phases/fraction of cells in G1 phase) of AT-101-treated cells compared to untreated ones (control) (Figure 4D). Earlier studies showed that AT-101 exhibit this effect on cell cycle through regulating the expression of retinoblastoma (Rb) and

cyclin Dl, which are cell cycle regulatory proteins.[35] Results collectively show that AT-101 triggers apoptotic cell death that increases with the increase in AT-101 dose and incubation time. Further, AT-101 reduces cell growth by inhibiting mitotic cell divisions and arresting the cell cycle.

Combined Effect of AT-101 and "Smart" Anti-Bcl-2 Particles on Cell Survival

We investigated the effect of combing low concentration of AT-101 (IC_{25}) with "smart" anti-Bcl-2 particles on the viability of UM-SCC-17B cancer cells. Results show that incubation of UM-SCC-17B cells with IC_{25} of AT-101 reduces the number of viable cells by 23% and 21% (i.e. 77% and 79% viable cells) compared to untreated cells (control) 48 and 72 hours after the treatment (Figure 5). Despite of the observed knockdown in the Bcl-2 mRNA and protein levels observed upon treatment of UM-SCC-17B cells with "smart" particles loaded with anti-Bcl-2 siRNA at a siRNA concentration of 100 nM (Figure 2), no change in cell viability was observed 48 and 72 hours after the treatment compared to untreated cells (data not shown). These results are in agreement with previously published reports, which show that inhibition of anti-apoptotic Bcl-2 protein expression alone does not influence the proliferation, cell cycle distribution, or apoptosis in MCF-7 breast cancer and HeLa cervical cancer cells.[36, 37] Significant reduction in cell viability is observed only after treatment with a much higher concentration (0.5 – 1 mM) of anti-Bcl2 siRNA[38], which is 5- to 10-fold higher than the concentration used in our study (100 nM). In comparison, treatment of UM-SCC-17B cells with "smart" particles loaded with anti-Bcl-2 siRNA at a siRNA concentration of 100 nM followed by incubation with the IC_{25} of AT-101 reduced the fraction of surviving cells to 37% and 25% after incubating for 48 and 72 hours, respectively (Figure 5). Treatment of UM-SCC-17B cells with "smart" particles loaded with scrambled siRNA followed by incubation with the IC_{25} of AT-101 did not affect cell viability compared to single treatment with AT-101 alone (Figure 5). Using the CalcuSyn Software, we calculated the Combinatorial Index (CI) when treating UM-SCC-17B cancer cells with a low dose of AT-101 (IC_{25}) and "smart" anti-Bcl-2 particles, which yielded a CI < 0.9 indicating a synergistic effect in reducing cell viability.

Treatment of UM-SCC-17B cells with a low dose of AT-101 (IC_{25}) caused a slight increase in the fraction of apoptotic cells to 4% compared to untreated (control) cells (Figure 6A). Combining AT-101 treatment with "smart" anti-Bcl-2 particles statistically increased the fraction of apoptotic UM-SCC-17B cancer cells to 12% and 14% after 48 and 72 hours, respectively (Figure 6A). Combined treatment of UM-SCC-17B cells with AT-101 and "smart" anti-Bcl-2 particles increased the cell fraction in G1 phase to 75%-76% compared to 59%-64% observed with single AT-101 treatment after 48 and 72 hours (Figure 6B & 6C). Further, the combined treatment of UM-SCC-17B cells with AT-101 and "smart" anti-Bcl-2 particles decreased the fraction of cells in S and G2 phases compared to that observed with single AT-101 treatment (Figure 6B & 6C). Results show that the mitotic index (S+G2/G1) of UM-SCC-17B cells is substantially reduced by the combined treatment of AT-101 and "smart" anti-Bcl-2 particles compared to single AT-101 treatment (Figure 6D). Results indicate that siRNA-mediated knockdown of anti-apoptotic Bcl-2 expression coupled with a low dose of AT-101 arrests cancer cell mitosis, decrease cell viability, and increase the

fraction of apoptotic cells, which indicate the potential of this therapeutic combination for treatment of head and neck cancer.

Conclusions

In summary, we used degradable, star-shaped β-CD-P(HMA-*co*-DMAEMA-*co*-TMAEMA)$_{4.8}$ polymer to condense anti-Bcl-2 siRNA forming pH-sensitive and membrane-destabilizing particles. “Smart” particles proved to deliver their cargo past the endosomal membrane and into the cytoplasm of UM-SCC-17B head and neck cancer cells, which triggered selective knockdown of anti-apoptotic Bcl-2 expression at the mRNA and protein levels. Treatment of UM-SCC-17B cells with AT-101 (Bcl-2 inhibitor) caused a dose-dependent inhibition in cancer cell viability and increase in the fraction of apoptotic cells. Combined treatment of UM-SCC-17B cells with a low dose of AT-101 (IC_{25}) and “smart” particles loaded with anti-Bcl-2 siRNA caused a substantial reduction in cancer cell viability and an increase in the apoptosis of cancer cells indicating a synergistic therapeutic effect. These results collectively indicate the potential benefit of combining siRNA-mediated knockdown of anti-apoptotic Bcl-2 protein expression with AT-101 (small molecule Bcl-2 inhibitor) for eradication of head and neck cancer cells.

Supplementary Material

Refer to Web version on PubMed Central for supplementary material.

Acknowledgments

This research is partially funded by Susan G. Komen Breast Cancer Foundation grant to Mohamed E.H. ElSayed and grant number P50-CA-97248 (University of Michigan Head and Neck SPORE) from the NIH/NCI and R01-DE23220 from the NIH/NIDCR to Jacques E. Nör. The authors would like to thank Dr. Zhaocheng Zhang and Atsushi Imai for their technical assistance.

References

1. Argiris A, Karamouzis MV, Raben D, Ferris RL. Head and neck cancer. Lancet. 2008; 371(9625): 1695–1709. [PubMed: 18486742]
2. Jemal A, Siegel R, Xu JQ, Ward E. Cancer Statistics, 2010. Ca-a Cancer Journal for Clinicians. 2010; 60(5):277–300. [PubMed: 20610543]
3. Adelstein DJ, Li Y, Adams GL, Wagner H Jr, Kish JA, Ensley JF, Schuller DE, Forastiere AA. An intergroup phase III comparison of standard radiation therapy and two schedules of concurrent chemoradiotherapy in patients with unresectable squamous cell head and neck cancer. Journal of Clinical Oncology. 2003; 21(1):92–8. [PubMed: 12506176]
4. Cooper JS, Pajak TF, Forastiere AA, Jacobs J, Campbell BH, Saxman SB, Kish JA, Kim HE, Cmelak AJ, Rotman M, Machtay M, Ensley JF, Chao KS, Schultz CJ, Lee N, Fu KK. Postoperative concurrent radiotherapy and chemotherapy for high-risk squamous-cell carcinoma of the head and neck. N Engl J Med. 2004; 350(19):1937–44. [PubMed: 15128893]
5. Galluzzi L, S L, Vitale I, Michels J, Martins I, Kepp O, Castedo M, Kroemer G. Molecular mechanisms of cisplatin resistance. Oncogene. 2012; 31(15):1869–1883. [PubMed: 21892204]
6. Wang SJ, Bourguignon LYW. Role of Hyaluronan-Mediated CD44 Signaling in Head and Neck Squamous Cell Carcinoma Progression and Chemoresistance. The American Journal of Pathology. 2011; 178(3):956–963. [PubMed: 21356346]
7. Djeu, JY.; Wei, S. Clusterin and Chemoresistance. In: George, FVW., editor. Advances in Cancer Research. Vol. 105. Academic Press; 2009. p. 77-92.

8. Bussink J, van der Kogel AJ, Kaanders JHAM. Activation of the PI3-K/AKT pathway and implications for radioresistance mechanisms in head and neck cancer. The Lancet Oncology. 2008; 9(3):288–296. [PubMed: 18308254]
9. Adams JM, Cory S. The Bcl-2 protein family: arbiters of cell survival. Science. 1998; 281(5381): 1322–6. [PubMed: 9735050]
10. Adams JM, Cory S. The Bcl-2 apoptotic switch in cancer development and therapy. Oncogene. 2007; 26(9):1324–37. [PubMed: 17322918]
11. dos Santos LV, Carvalho AL. Bcl-2 targeted-therapy for the treatment of head and neck squamous cell carcinoma. Recent Pat Anticancer Drug Discov. 2011; 6(1):45–57. [PubMed: 21110823]
12. Reed JC. Mechanisms of apoptosis avoidance in cancer. Curr Opin Oncol. 1999; 11(1):68–75. [PubMed: 9914881]
13. Reed JC. Dysregulation of apoptosis in cancer. Journal of Clinical Oncology. 1999; 17(9):2941–53. [PubMed: 10561374]
14. Kaufmann SH, Gores GJ. Apoptosis in cancer: cause and cure. Bioessays. 2000; 22(11):1007–17. [PubMed: 11056477]
15. Gallo O, Boddi V, Calzolari A, Simonetti L, Trovati M, Bianchi S. bcl-2 protein expression correlates with recurrence and survival in early stage head and neck cancer treated by radiotherapy. Clin Cancer Res. 1996; 2(2):261–7. [PubMed: 9816168]
16. Sharma H, Sen S, Mathur M, Bahadur S, Singh N. Combined evaluation of expression of telomerase, survivin, and anti-apoptotic Bcl-2 family members in relation to loss of differentiation and apoptosis in human head and neck cancers. Head Neck. 2004; 26(8):733–40. [PubMed: 15287041]
17. Zeitlin BD, Nör JE. Small-molecule inhibitors reveal a new function for Bcl-2 as a proangiogenic signaling molecule. Current Topics in Microbiology and Immunology. 2011; 348:115–137. [PubMed: 20941592]
18. Imai A, Zeitlin BD, Visioli F, Dong ZH, Zhang ZC, Krishnamurthy S, Light E, Worden F, Wang SM, Nor JE. Metronomic Dosing of BH3 Mimetic Small Molecule Yields Robust Antiangiogenic and Antitumor Effects. Cancer Research. 2012; 72(3):716–725. [PubMed: 22158856]
19. Liu G, Kelly WK, Wilding G, Leopold L, Brill K, Somer B. An Open-Label Multicenter, Phase I/II Study of Single-Agent AT-101 in Men with Castrate-Resistant Prostate Cancer. Clinical Cancer Research. 2009; 15(9):3172–3176. [PubMed: 19366825]
20. El-Sharaky AS, Newairy AA, Elguindy NM, Elwafa AA. Spermatotoxicity, biochemical changes and histological alteration induced by gossypol in testicular and hepatic tissues of male rats. Food and Chemical Toxicology. 2010; 48(12):3354–3361. [PubMed: 20832445]
21. Rinchard J, Ciereszko A, Dabrowski K, Ottobre J. Effects of gossypol on sperm viability and plasma sex steroid hormones in male sea lamprey, Petromyzon marinus. Toxicology Letters. 2000; 111(3):189–198. [PubMed: 10643862]
22. Hutchinson RW, Barhoumi R, Miles JM, Burghardt RC. Attenuation of Gossypol Cytotoxicity by Cyclic AMP in a Rat Liver Cell Line. Toxicology and Applied Pharmacology. 1998; 151(2):311–318. [PubMed: 9707507]
23. Teng CS. Gossypol-induced apoptotic DNA fragmentation correlates with inhibited protein kinase C activity in spermatocytes. Contraception. 1995; 52(6):389–395. [PubMed: 8749604]
24. Kaneko T, Zhang Z, Mantellini MG, Karl E, Zeitlin B, Verhaegen M, Soengas MS, Lingen M, Strieter RM, Nunez G, Nor JE. Bcl-2 orchestrates a cross-talk between endothelial and tumor cells that promotes tumor growth. Cancer Research. 2007; 67(20):9685–93. [PubMed: 17942898]
25. Sharma H, Sen S, Lo Muzio L, Mariggio A, Singh N. Antisense-mediateddownregulation of anti-apoptotic proteins induces apoptosis and sensitizes head and necksquamous cell carcinoma cells to chemotherapy. Cancer Biol Ther. 2005; 4(7):720–7. [PubMed: 15917659]
26. Durmaz YY, Lin YL, ElSayed MEH. Development of Degradable, pH-Sensitive,Star Vectors for Enhancing the Cytoplasmic Delivery of Nucleic Acids. Advanced FunctionalMaterials. 2013
27. Haddleton DM, Waterson C. Phenolic ester-based initiators for transition metal mediated living polymerization. Macromolecules. 1999; 32(26):8732–8739.

28. Etrych T, Chytil P, Jelinkova M, Rihova B, Ulbrich K. Synthesis of HPMA copolymers containing doxorubicin bound via hydrazone linkage. Effect of spacer on drug release and in vitro cytotoxicity. Mocromol Biosci. 2002; 2(1):43–52.
29. Ulbrich K, Etrych T, Chytil P, Jelínková M, Říhová B. HPMA copolymers with pH-controlled release of doxorubicin: in vitro cytotoxicity and in vivo antitumor activity. J Control Release. 2003; 87(1-3):33–47. [PubMed: 12618021]
30. Lin YL, Jiang G, Birrell LK, El-Sayed ME. Degradable, pH-sensitive, membrane-destabilizing, comb-like polymers for intracellular delivery of nucleic acids. Biomaterials. 2010; 31(27):7150–66. [PubMed: 20579726]
31. Neiva KG, Zhang Z, Miyazawa M, Warner KA, Karl E, Nor JE. Cross talk initiated by endothelial cells enhances migration and inhibits anoikis of squamous cell carcinoma cells through STAT3/Akt/ERK signaling. Neoplasia. 2009; 11(6):583–93. [PubMed: 19484147]
32. Buck AC, Shen CX, Schirrmeister H, Schmid-Kotsas A, Munzert G, Guhlmann A, Mehrke G, Klug N, Gross HJ, Bachem M, Reske SN. Liposomal delivery of antisense oligonucleotides for efficient downregulation of Bcl-2 and induction of apoptosis. Cancer Biotherapy and Radiopharmaceuticals. 2002; 17(3):281–289. [PubMed: 12136520]
33. Oliver CL, Bauer JA, Wolter KG, Ubell ML, Narayan A, O'Connell KM, Fisher SG, Wang S, Wu X, Ji M, Carey TE, Bradford CR. In vitro effects of the BH3 mimetic, (-)-gossypol, on head and neck squamous cell carcinoma cells. Clin Cancer Res. 2004; 10(22):7757–63. [PubMed: 15570010]
34. Ashimori N, Zeitlin BD, Zhang Z, Warner K, Turkienicz IM, Spalding AC, Teknos TN, Wang S, Nor JE. TW-37, a small-molecule inhibitor of Bcl-2, mediates S-phase cell cycle arrest and suppresses head and neck tumor angiogenesis. Mol Cancer Ther. 2009; 8(4):893–903. [PubMed: 19372562]
35. Ligueros M, Jeoung D, Tang B, Hochhauser D, Reidenberg MM, Sonenberg M. Gossypol inhibition of mitosis, cyclin D1 and Rb protein in human mammary cancer cells and cyclin-D1 transfected human fibrosarcoma cells. Br J Cancer. 1997; 76(1):21–8. [PubMed: 9218727]
36. Yde CW, Issinger OG. Enhancing cisplatin sensitivity in MCF-7 human breast cancer cells by down-regulation of Bcl-2 and cyclin D1. International Journal of Oncology. 2006; 29(6):1397–1404. [PubMed: 17088977]
37. Huang SL, Wu Y, Yu H, Zhang P, Zhang XQ, Ying L, Zhao HF. Inhibition of Bcl-2 expression by a novel tumor-specific RNA interference system increases chemosensitivity to 5-fluorouracil in Hela cells. Acta pharmacologica Sinica. 2006; 27(2):242–248. [PubMed: 16412276]
38. Vestin A, Khazanov E, Avni D, Sergeyev V, Barenholz Y, Sidi Y, Yakobson E. siRNA-Lipoplex-Mediated Bcl-2 and Bcl-xL Gene Silencing Induces Apoptosis in MCF-7 Human Breast Carcinoma Cells. The Open Chemical and Biomedical Methods Journal. 2008; 1:28–43.

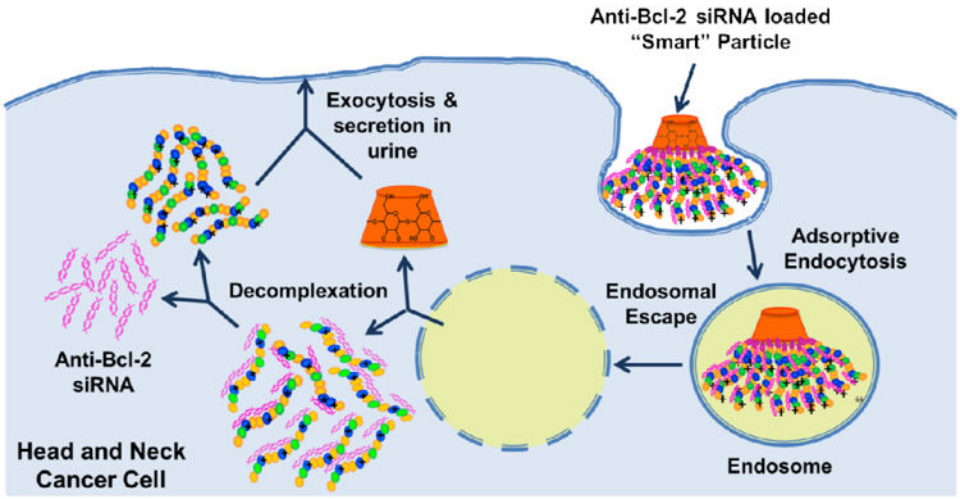

Figure 1.

A schematic drawing showing internalization of anti-Bcl-2 siRNA loaded "smart" particles by adsorptive endocytosis. In the endosome, acid-labile hydrazone linkages are hydrolyzed in response to acidic pH and release the membrane-active P(HMA-*co*-DMAEMA-*co*-TMAEMA) grafts, which rupture the endosomal membrane and release the loaded siRNA cargo into the cytoplasm.

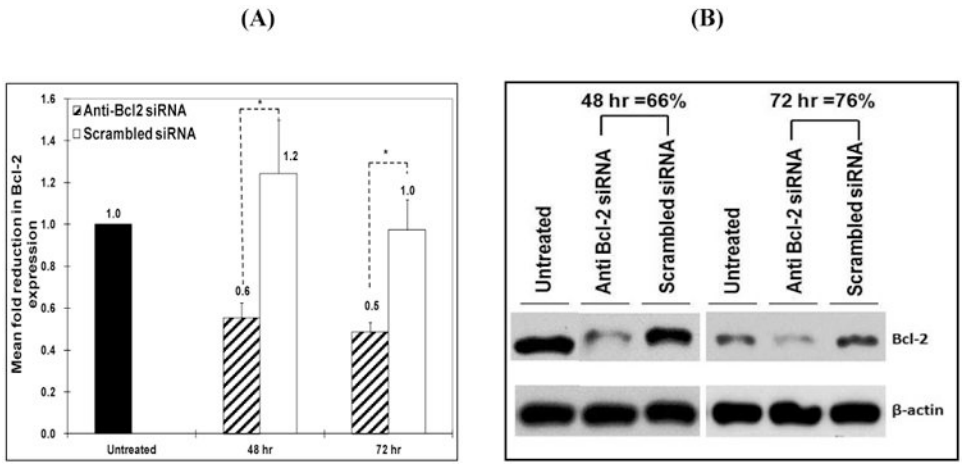

Figure 2.

Effect of "smart" particles prepared by complexation of β-CD-P(HMA-*co*-DMAEMA-*co*-TMAEMA)$_{4.8}$ polymer with 0.57 μg of the anti-Bcl-2 or scrambled siRNA at an N/P (+/-) ratio of 2.5/1 on (A) Bcl-2 mRNA and (B) protein levels in UM-SCC-17B head and neck cancer cells after 48 and 72 hours. Bcl-2 mRNA levels are normalized to that of 18S rRNA. Results are the average + the standard error of the mean of five replicates. Statistical difference between "smart" particles loaded with anti-Bcl-2 and scrambled siRNA was evaluated using paired *t* test where * denotes $p \leq 0.05$. Bcl-2 protein levels are quantified using Image J software (NIH, Bethesda, MD) and normalized to the levels of β-actin at similar time points.

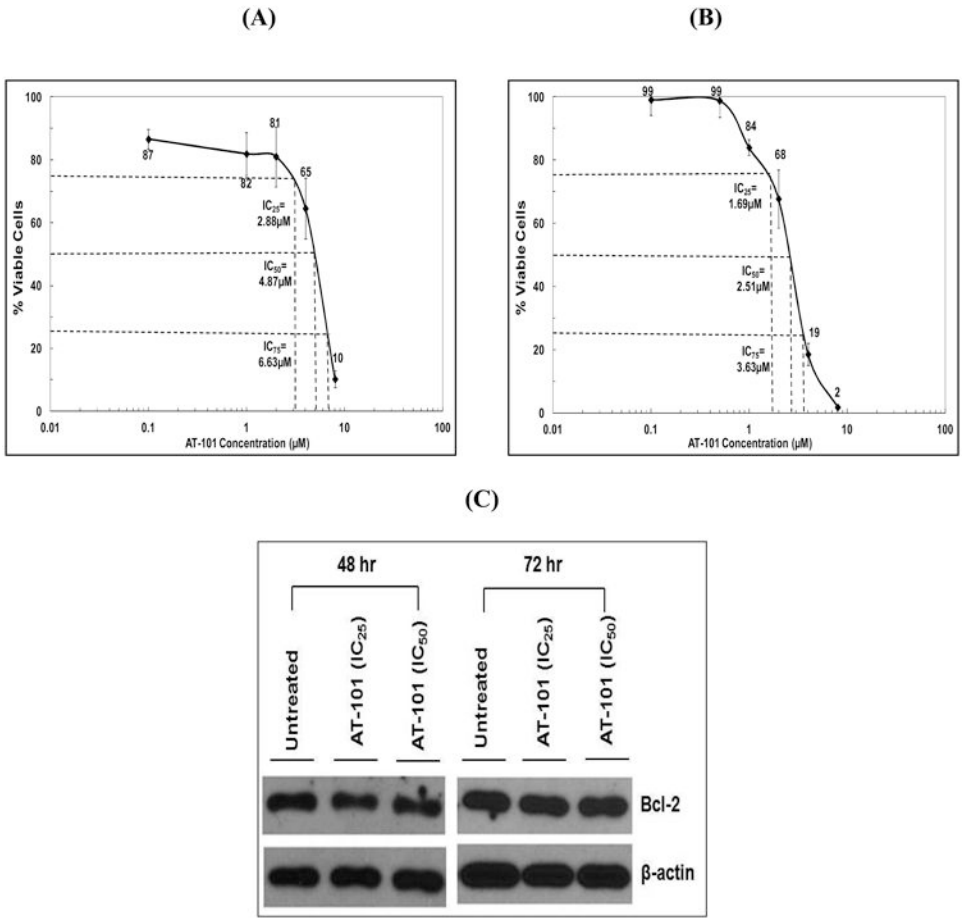

Figure 3.

Effect of concentration (0, 0.1, 0.5, 1, 2, 4, and 8 μM) of AT-101 inhibitor on the viability of UM-SCC-17B cancer cells upon incubation for (A) 48 and (B) 72 hours determined using the SRB assay. Results are the average ± the standard error of the mean of triplicates. Effect of incubating UM-SCC-17B cancer cells with the IC_{25} and IC_{50} of AT-101 inhibitor for 48 and 72 hours on Bcl-2 protein level compared to untreated (control) cells.

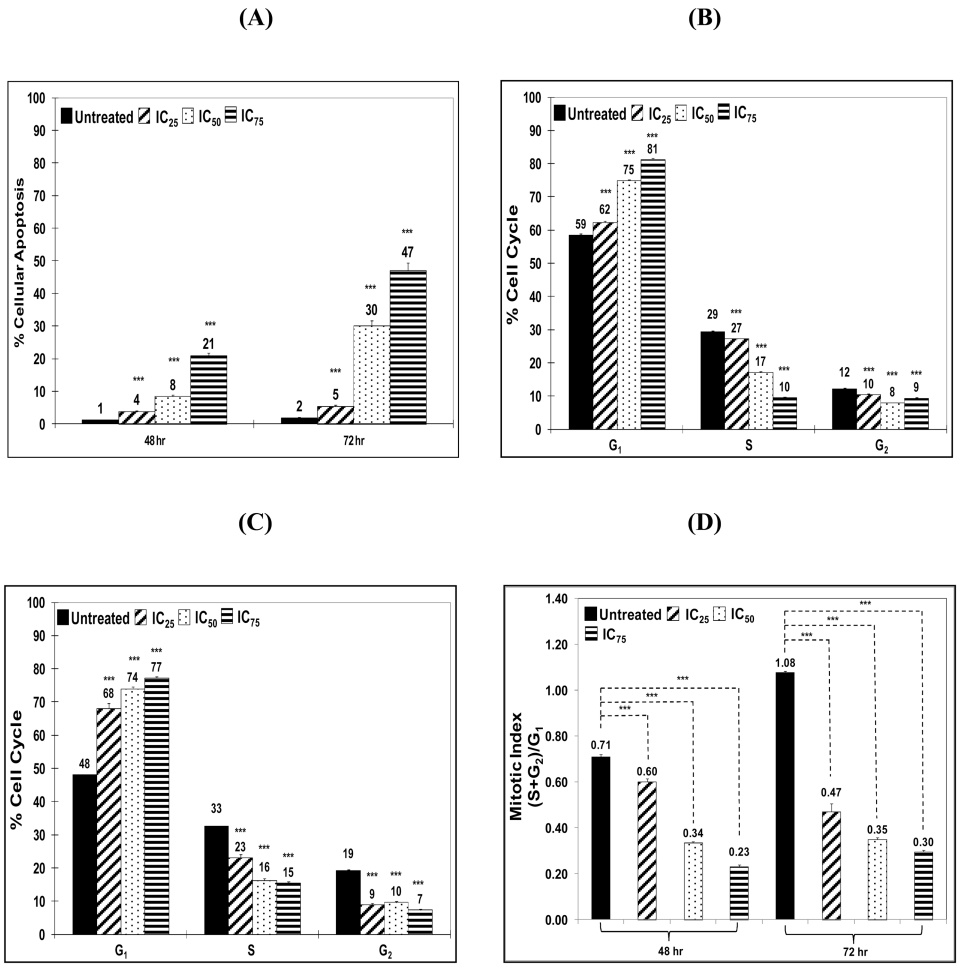

Figure 4.

(A) Relationship between AT-101 dose on the fraction of apoptotic UM-SCC-17B cancer cells after 48 and 72 hours. The percentage of UM-SCC-17B cancer cells in G1, S, and G2 phases after treatment with IC_{25}, IC_{50}, and IC_{75} of AT-101 for 24 hours (B) and 72 hours (C), which was used to calculate the mitotic index at both time points (D). Results are the average + the standard error of the mean of five replicates. Statistical difference between the surviving fraction of UM-SCC-17B cells after treatment with different concentrations of AT-101 compared to untreated (control) cells was evaluated using paired *t* test where *** denotes $p \leq 0.005$.

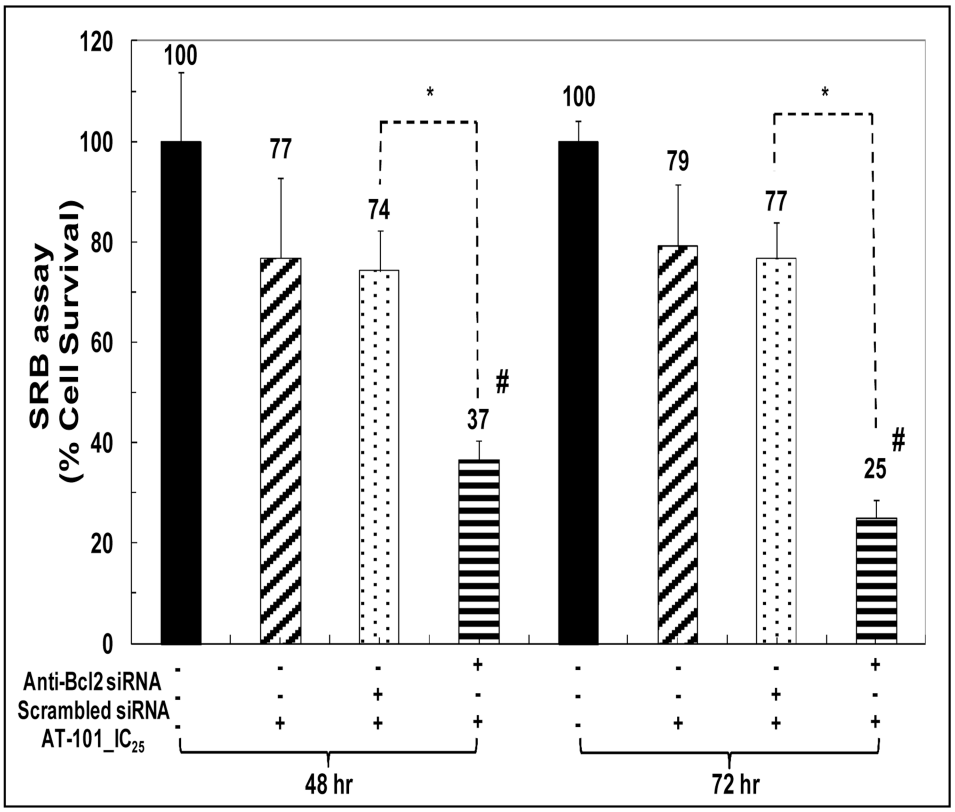

Figure 5.

Effect of the IC_{25} of AT-101 alone and combined with "smart" particles loaded with anti-Bcl-2 or scrambled siRNA on the viability of UM-SCC-17B cancer cells after incubation for 48 and 72 hours. Results are the average + the standard error of the mean of triplicates. Statistical difference between the surviving fraction of UM-SCC-17B cells after treatment with AT-101 combined with "smart" particles loaded with anti-Bcl-2 siRNA compared to those treated with an equal dose of AT-101 and "smart" particles loaded with scrambled siRNA was evaluated using paired *t* test where * denotes $p \leq 0.05$. The # denotes a synergistic effect (i.e. Combinatorial Index < 0.9) upon combining AT-101 with "smart" anti-Bcl-2 particles.

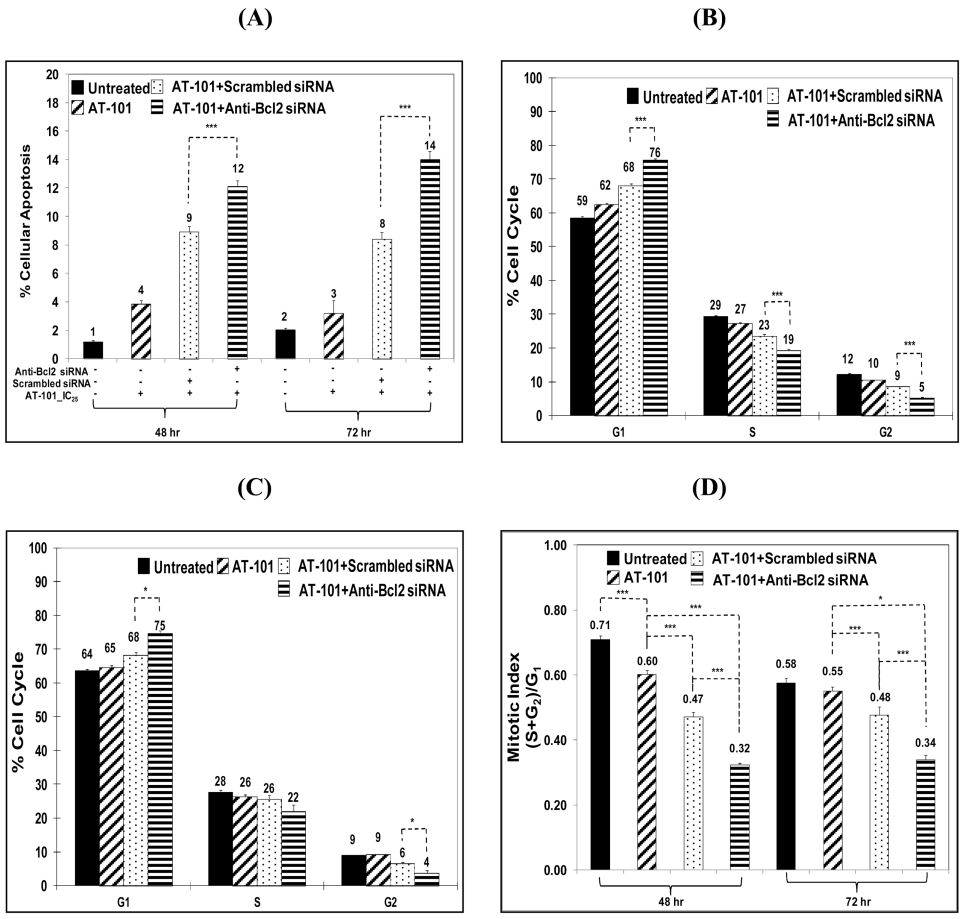

Figure 6.

(A) Change in the fraction of apoptotic UM-SCC-17B cancer cells upon incubation with the IC_{25} of AT-101 alone or in combination with "smart" particles loaded with anti-Bcl-2 or scrambled siRNA for 48 and 72 hours. The percentage of UM-SCC-17B cancer cells in G1, S, and G2 phases after treatment with IC_{25} of AT-101 alone and in combination with "smart" particles loaded with anti-Bcl-2 or scrambled siRNA after incubation for 48 hours (B) and 72 hours (C), which was used to calculate the mitotic index at both time points (D). Results are the average + the standard error of the mean of five replicates. Statistical difference between different treatments was evaluated using paired *t* test where * denotes $p \leq 0.05$ and *** denotes $p \leq 0.005$.